AMERICAN SOCIETY FOR MICROBIOLOGY | Journal of Virology®

VIRUS-CELL INTERACTIONS

African Swine Fever Virus Cysteine Protease pS273R Inhibits Type I Interferon Signaling by Mediating STAT2 Degradation

Yu-Hui Li,[a,b,c] Jiang-Ling Peng,[d,e] Zhi-Sheng Xu,[a] Mei-Guang Xiong,[a,b,c] Huang-Ning Wu,[a,b,c] Su-Yun Wang,[a,b] Dan Li,[d,e] Guo-Qiang Zhu,[d,e] Yong Ran,[a,b] Yan-Yi Wang[a,b]

[a]Key Laboratory of Special Pathogens and Biosafety, Wuhan Institute of Virology, Center for Biosafety Mega-science, Chinese Academy of Sciences, Wuhan, China
[b]African Swine Fever Regional Laboratory of China, Wuhan Institute of Virology, Chinese Academy of Sciences, Wuhan, China
[c]University of Chinese Academy of Sciences, Beijing, China
[d]State Key Laboratory of Veterinary Etiological Biology, OIE/National Foot and Mouth Disease Reference Laboratory, Lanzhou Veterinary Research Institute, Chinese Academy of Agricultural Sciences, Lanzhou, China
[e]African Swine Fever Regional Laboratory, Lanzhou Veterinary Research Institute, Chinese Academy of Agricultural Sciences, Lanzhou, China

Yu-Hui Li and Jiang-Ling Peng contributed equally to this work. Author order was determined in order of decreasing seniority.

ABSTRACT African swine fever virus (ASFV) is a large DNA virus that causes African swine fever (ASF), an acute and hemorrhagic disease in pigs with lethality rates of up to 100%. To date, how ASFV efficiently suppress the innate immune response remains enigmatic. In this study, we identified ASFV cysteine protease pS273R as an antagonist of type I interferon (IFN). Overexpression of pS273R inhibited JAK-STAT signaling triggered by type I IFNs. Mechanistically, pS273R interacted with STAT2 and recruited the E3 ubiquitin ligase DCST1, resulting in K48-linked polyubiquitination at K55 of STAT2 and subsequent proteasome-dependent degradation of STAT2. Furthermore, such a function of pS273R in JAK-STAT signaling is not dependent on its protease activity. These findings suggest that ASFV pS273R is important to evade host innate immunity.

IMPORTANCE ASF is an acute disease in domestic pigs caused by infection with ASFV. ASF has become a global threat with devastating economic and ecological consequences. To date, there are no commercially available, safe, and efficacious vaccines to prevent ASFV infection. ASFV has evolved a series of strategies to evade host immune responses, facilitating its replication and transmission. Therefore, understanding the immune evasion mechanism of ASFV is helpful for the development of prevention and control measures for ASF. Here, we identified ASFV cysteine protease pS273R as an antagonist of type I IFNs. ASFV pS273R interacted with STAT2 and mediated degradation of STAT2, a transcription factor downstream of type I IFNs that is responsible for induction of various IFN-stimulated genes. pS273R recruited the E3 ubiquitin ligase DCST1 to enhance K48-linked polyubiquitination of STAT2 at K55 in a manner independent of its protease activity. These findings suggest that pS273R is important for ASFV to escape host innate immunity, which sheds new light on the mechanisms of ASFV immune evasion.

KEYWORDS African swine fever virus, pS273R, type I interferon, STAT2

African swine fever (ASF) is an acute hemorrhagic disease that is fatal to wild and domestic pigs, with mortality rates of up to 100%. It is caused by infection with African swine fever virus (ASFV), which was first reported in Africa in the 1920s (1). Due to the absence of effective vaccines, ASF has been spreading in Europe and Asia in recent decades (2), becoming a global threat with devastating economic and ecological consequences.

ASFV is a large DNA virus belonging to the *Asfivirus* genus of the *Asfaviridae* family. It has a large genome of around 170 to 190 kb and encodes more than 150 proteins,

Editor Bryan R. G. Williams, Hudson Institute of Medical Research

Address correspondence to Yong Ran, ranyong@wh.iov.cn, or Yan-Yi Wang, wangyy@wh.iov.cn.

The authors declare no conflict of interest.

Received 22 December 2022
Accepted 2 February 2023
Published 1 March 2023

including essential factors required for genome replication and transcription and proteins that play various roles in manipulation of the host immune responses (3–5). Multiple ASFV-encoded proteins have been reported to be involved in immune evasion. For example, ASFV A238L inhibits the activation of the transcription factors nuclear factor κB (NF-κB), c-Jun, and nuclear factor of activated T cells (NFAT) (6, 7), while ASFV A276R inhibits the activation of the transcription factor interferon (IFN) regulatory factor 3 (IRF3) (8). ASFV I267L and DP96R prevent IFN-β production by inhibiting the RNA polymerase III-retinoic acid-inducible gene I (RIG-I) pathway and the cyclic GMP-AMP synthase (cGAS)-stimulator of IFN genes (STING) pathway, respectively (9, 10).

Type I IFNs play important roles in antiviral responses via the effects of various IFN-stimulated genes (ISGs) that are induced by the Janus kinase (JAK)-signal transducer and activator of transcription (STAT) pathway. Binding of type I IFNs to their receptors leads to receptor tyrosine phosphorylation by JAK1 and tyrosine kinase 2 (TYK2). Subsequently, activated JAK1 and TYK2 phosphorylate the transcription factors STAT1 and STAT2, leading to assembly of the ISG factor 3 (ISGF3) heterotrimer, which is formulated by phosphorylated STAT1, STAT2, and IFN regulatory factor 9 (IRF9) in cytoplasm. ISGF3 is then translocated to the nucleus, binds to IFN-stimulated response elements (ISREs), and initiates the transcription of various ISGs (11). It has been reported that multigene family 360 (MGF360) and MGF530/505 of ASFV are involved in modulation of the type I IFN responses (12).

In this study, we screened ~150 independent cDNA expression clones of ASFV by reporter assays. We found that ASFV pS273R inhibited type I IFN-triggered signaling. pS273R is encoded by the S273R gene and belongs to the small ubiquitin-like modifier protein (SUMO-1)-specific protease family (13). It has been reported that pS273R functions as a cysteine protease that processes polyprotein precursors to mature structural proteins required for virus assembly. For example, the polyprotein pp220 is cleaved by pS273R to yield p5, p34, p14, p37, and p150, while the polyprotein pp62 is cleaved by pS273R to yield p15, p35, and p8 (14). In our study, we uncover the immune evasion function of pS273R. We demonstrate that pS273R interacts with STAT2 and enhances K48-linked polyubiquitination and degradation of STAT2 by recruiting the E3 ubiquitin ligase DCST1 and thus impairs type I IFN-mediated antiviral effects.

RESULTS

ASFV pS273R inhibits JAK-STAT signaling induced by type I IFNs. Type I IFNs are important for the host antiviral defense. To identify potential candidate ASFV proteins that could antagonize type I IFN-induced signaling, we screened ~150 independent cDNA expression clones of ASFV by reporter assays. In this screening, we identified pS273R as a potent antagonist of type I IFN signaling (see Fig. S1 in the supplemental material). Overexpression of pS273R inhibited activation of the STAT1/2 reporter by IFN-β stimulation (Fig. 1A). However, pS273R showed little effect on IRF1 activation stimulated by IFN-γ (Fig. 1B). Consistently, overexpression of pS273R impaired the transcription of *ISG15*, *ISG54*, and *ISG56* genes in response to IFN-β treatment in HEK293T cells (Fig. 1C). To further confirm the function of pS273R in porcine cells, we established PK-15 cells stably expressing pS273R and found that pS273R also inhibited transcription of *Mx2*, *Isg15*, and *Isg54* genes stimulated by porcine IFN-α (Fig. 1D). It is well known that phosphorylations of JAK1, TYK2, STAT1, and STAT2 are key events in the activation of JAK-STAT signaling stimulated by type I IFNs. We found that pS273R impaired phosphorylation of STAT1 and STAT2 in HEK293T and PK-15 cells (Fig. 1E and F) but had little effect on phosphorylation of JAK1 and TYK2 (Fig. 1E). In these experiments, we also noticed that the level of STAT2 in cells expressing pS273R was lower than that in the control cells (Fig. 1E and F).

ASFV pS273R interacts with STAT2 and induces STAT2 degradation. Based on these results, we further investigated whether pS73R inhibited type I IFN-induced signaling by targeting STAT2. In coimmunoprecipitation experiments, pS273R interacted with STAT2 but not JAK1, TYK2, STAT1, or IRF9 (Fig. 2A; also see Fig. S1B). Consistently, pS273R was associated with endogenous porcine STAT2 following ASFV infection (Fig. 2B). In addition, *in vitro* pulldown assays with purified recombinant STAT2 and pS273R

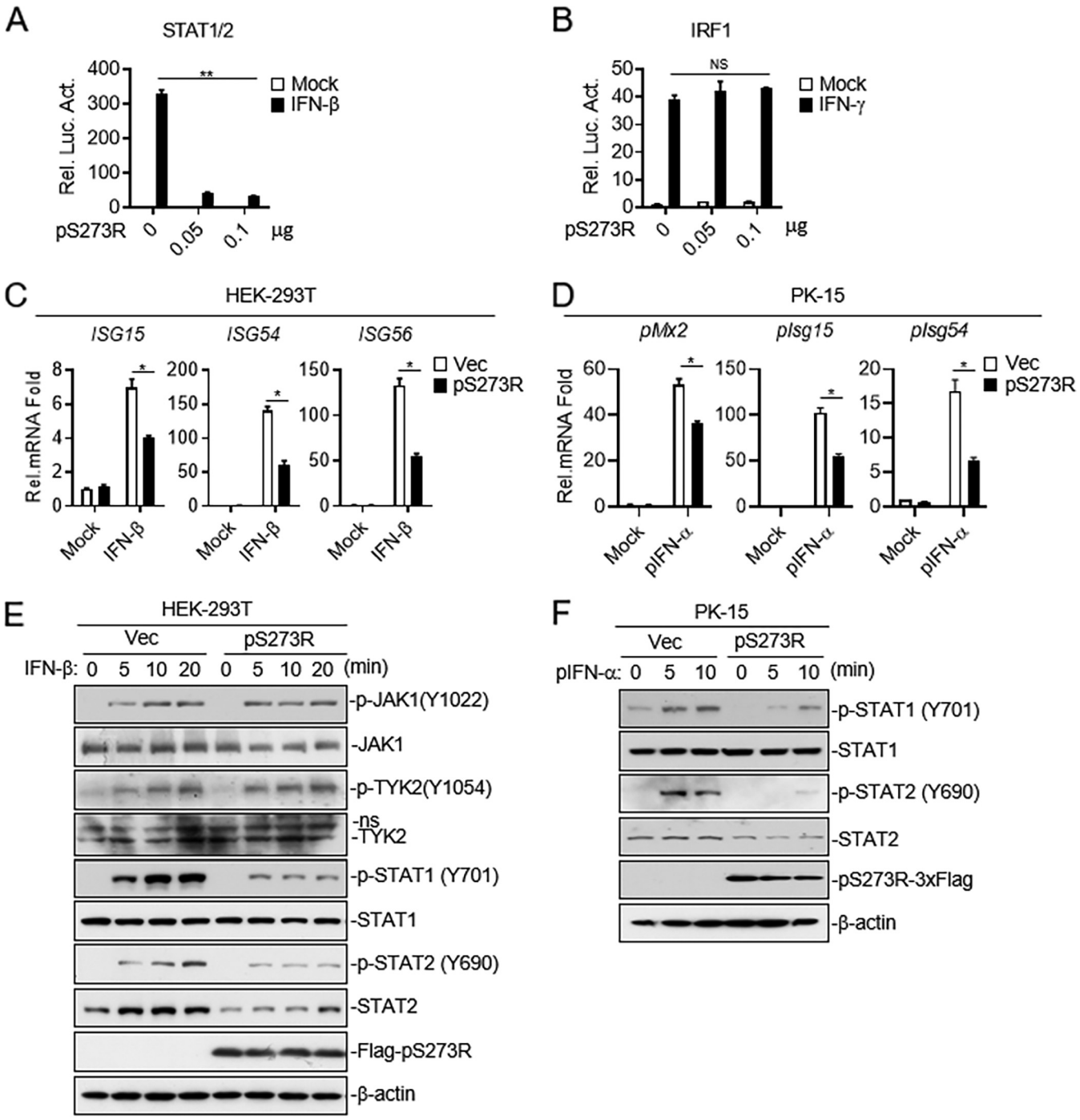

FIG 1 ASFV pS273R inhibits JAK-STAT signaling induced by type I IFNs. (A) HEK293T cells were transfected with expression plasmids for pS273R, STAT1/2 luciferase reporter (0.01 μg), and thymidine kinase (TK) reporter (0.01 μg/mL). Twenty-four hours later, cells were stimulated with IFN-β (20 μM) for 10 h before luciferase assays were performed. One-way ANOVA was used for statistical analysis for means and average deviations. Data shown are representative of 4 repeated experiments. (B) HEK293T cells were transfected with plasmids of the IRF1 luciferase reporter (0.05 μg) and TK reporter (0.01 μg/mL). Twenty-four hours later, cells were stimulated with IFN-γ (20 μM) for 10 h before luciferase assays were performed. One-way ANOVA was used for statistical analysis for means and average deviations. Data shown are representative of 2 repeated experiments. (C) HEK293T cells were transfected with pS273R. Twenty-four hours later, cells were stimulated with IFN-β (20 μM) for 6 h. The *ISG15*, *ISG54*, and *ISG56* mRNA levels were analyzed by reverse transcription (RT)-qPCR. Student's *t* test was used for statistical analysis for means and average deviations. Data shown are representative of 3 repeated experiments. (D) PK-15 cells stably expressing pS273R were stimulated with porcine IFN-α (400 U) for 6 h. The porcine *Mx2*, *Isg15*, and *Isg54* mRNA levels were analyzed by RT-qPCR. Student's *t* test was used for statistical analysis for means and average deviations. Data shown are representative of 2 repeated experiments. (E) HEK293T cells (5×10^6) were transfected with Flag-tagged pS273R (1 μg). Twenty-four hours later, cells were stimulated with IFN-β (20 μM) for 0, 5, 10, or 20 min before Western blot assays were performed. Data shown are representative of 3 repeated experiments. (F) PK-15 cells stably expressing pS273R were stimulated with porcine IFN-α (400 U) for 0, 5, or 10 min before Western blot assays were performed with the indicated antibodies. Data shown are representative of 3 repeated experiments.

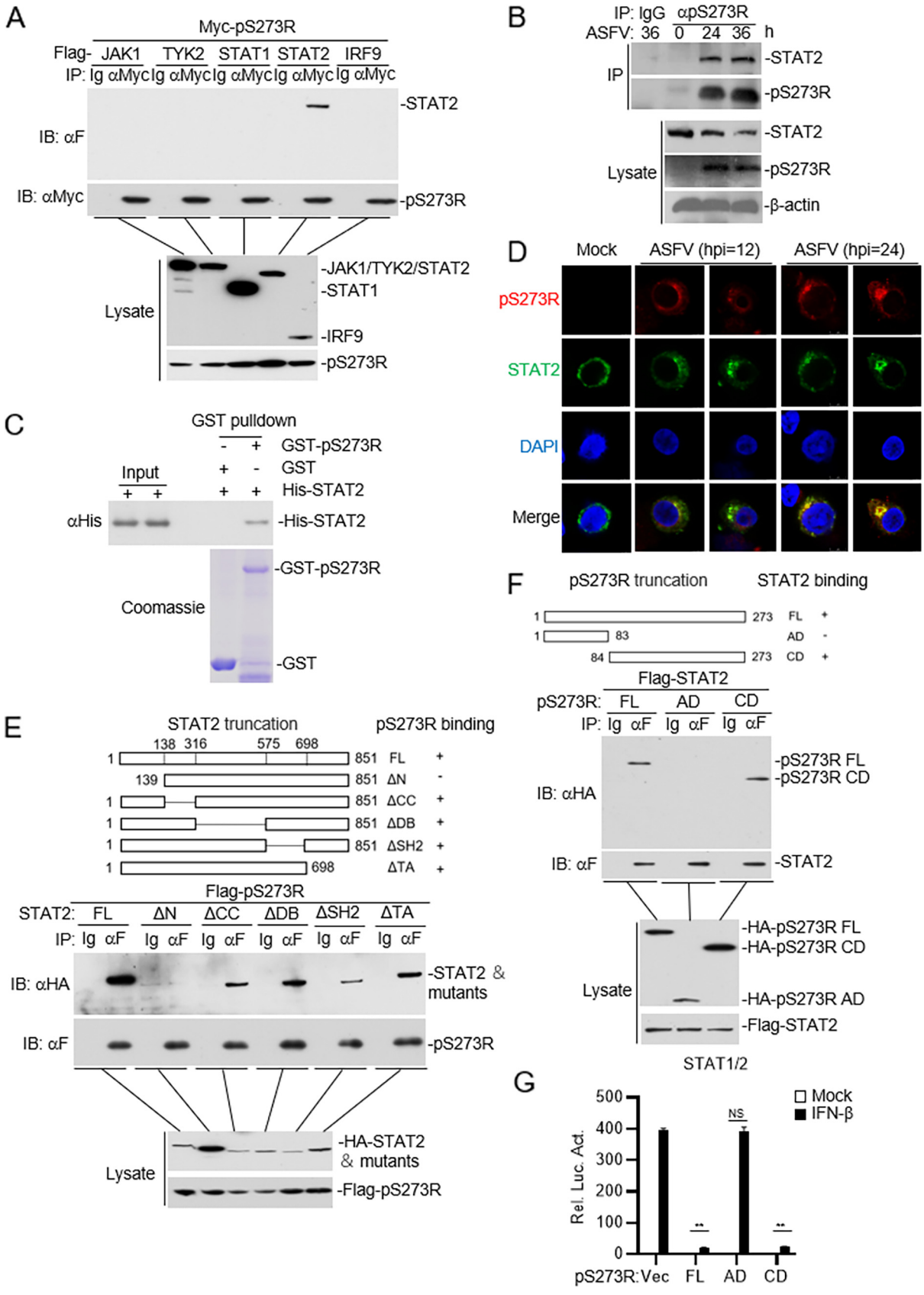

FIG 2 ASFV pS273R interacts with STAT2. (A) HEK293T cells (5×10^6) were cotransfected with Myc-tagged pS273R (5 μg) and Flag-tagged JAK1 (5 μg), Flag-tagged TYK2 (5 μg), Flag-tagged STAT1 (5 μg), Flag-tagged STAT2 (5 μg), or Flag-tagged IRF9 (5 μg). Coimmunoprecipitation and

(Continued on next page)

showed that pS273R bound to STAT2 directly (Fig. 2C). Confocal microscopy showed that STAT2 was dispersed through the cytosol in pulmonary alveolar macrophages (PAMs) under normal physiological conditions (Fig. 2D). Interestingly, after ASFV infection, STAT2 aggregated to form punctate structures in which it remarkably colocalized with pS273R, suggesting that pS273R is associated with STAT2 following ASFV infection (Fig. 2D). Moreover, we tried to determine which domains of STAT2 and pS273R are responsible for their interaction. Domain-mapping experiments indicated that the N-terminal domain of STAT2 and the core domain (CD) of pS273R were essential for their interaction (Fig. 2E and F). Consistently, the pS273R CD but not the arm domain of pS273R (AD) showed an inhibitory effect on IFN-β-stimulated activation of STAT1/2 (Fig. 2G). Taken together, these results suggest that pS273R interacts with STAT2 following ASFV infection.

Since overexpression of pS273R resulted in lower levels of STAT2, we further investigated whether pS273R affects STAT2 stability. In cotransfection experiments, we found that pS273R mediated STAT2 degradation in a dose-dependent manner but showed little effect on the stability of JAK1, TYK2, STAT1, or IRF9 (Fig. 3A). Consistently, while the expression of pS273R increased following ASFV infection, the relative level of STAT2 (the STAT2/β-actin ratio) decreased (Fig. 3B). In addition, pS273R-mediated degradation of STAT2 was completely inhibited by MG132, an inhibitor of the proteasome, instead of 3-methyladenine (3MA) or NH_4Cl, which are inhibitors of the lysosomal pathway and the autophagy pathway, respectively (Fig. 3C and D). Taken together, these results suggested that pS273R inhibits type I IFN signaling by inducing proteasome-dependent degradation of STAT2.

ASFV pS273R recruits the E3 ubiquitin ligase DCST1 and enhances K48-linked polyubiquitination of STAT2. Since ubiquitination is usually involved in proteasome-dependent protein turnover, we next examined whether pS273R enhanced the ubiquitination of STAT2, and we found that overexpression of pS273R markedly enhanced the polyubiquitination of STAT2 (Fig. 4A). To investigate which type of polyubiquitination of STAT2 was enhanced by pS273R, we transfected pS273R with wild-type ubiquitin or ubiquitin mutants such as K6O, K11O, K27O, K29O, K33O, K48O, and K63O, which contain only one lysine residue at the indicated position, with other lysine residues being substituted by arginines. We found that pS273R enhanced K48-linked polyubiquitination of STAT2 but had little effect on other types of polyubiquitination of STAT2 (Fig. 4B).

Previously, E3 ubiquitin ligases such as PDLIM2, DCST1, and FBXW7 have been reported to be involved in K48-linked polyubiquitination of STAT2 (15–17). Coimmunoprecipitation experiments showed that, while all three E3 ligases interacted with STAT2, only DCST1 and not PDLIM2 or FBXW7 could interact with pS273R (Fig. 4C; also see Fig. S2A). Notably, pS273R enhanced the interaction between STAT2 and DCST1 but showed no obvious effects on STAT2-PDLIM2 or STAT2-FBXW7 interactions (Fig. 4D; also see Fig. S2B). Furthermore, we examined whether the antagonistic function of pS273R is dependent on DCST1. The quantitative PCR (qPCR) results showed that impaired transcription of *Isg15*, *Isg54*, and *Oas1* mediated by pS273R was completely restored by knockdown of DCST1 in

FIG 2 Legend (Continued)
immunoblotting (IB) were performed with the indicated antibodies. Data shown are representative of 2 repeated experiments. (B) PAMs (1×10^7) were infected with ASFV CN/GS/2018 strain (MOI of 0.1) for 24 h or 36 h. Coimmunoprecipitation (IP) and immunoblotting were performed with the indicated antibodies. Data shown are representative of 2 repeated experiments. (C) *In vitro* pulldown assays were performed with the indicated antibodies and anti-GST-tagged beads using purified recombinant STAT2 and pS273R expressed in *E. coli* cells. Data shown are representative of 2 repeated experiments. (D) PAM cells (5×10^4) were infected with ASFV (MOI of 0.2) for 0, 12, or 24 h. STAT2 and pS273R were stained with anti-STAT2 antibody and anti-pS273R antibody. The nuclei were stained with DAPI. Confocal assays were performed by Nikon 100 microscopy. (E) HEK293T cells (5×10^6) were cotransfected with Flag-tagged pS273R (5 μg) and HA-tagged STAT2 or its truncation mutants (5 μg). The upper section shows schematic representations of STAT2 truncations. Coimmunoprecipitation and immunoblotting were performed with the indicated antibodies. Data shown are representative of 4 repeated experiments. (F) HEK293T cells (5×10^6) were cotransfected with Flag-tagged STAT2 (5 μg) and HA-tagged pS273R or its truncation mutants (5 μg). The upper section shows schematic representations of pS273R truncations. Coimmunoprecipitation and immunoblotting were performed with the indicated antibodies. Data shown are representative of 2 repeated experiments. Vec, vector; FL, full length; AD, AD of pS273R; CD, CD of pS273R. (G) HEK293T cells were transfected with plasmids of full length, AD or CD domain of pS273R, STAT1/2 luciferase reporter (0.01 μg) and TK reporter (0.01 μg). Twenty-four hours later, cells were stimulated with IFN-β (20 μM) for 10 hours before luciferase assays were performed. ONE-way ANOVA was used for statistical analysis for means and average deviations.

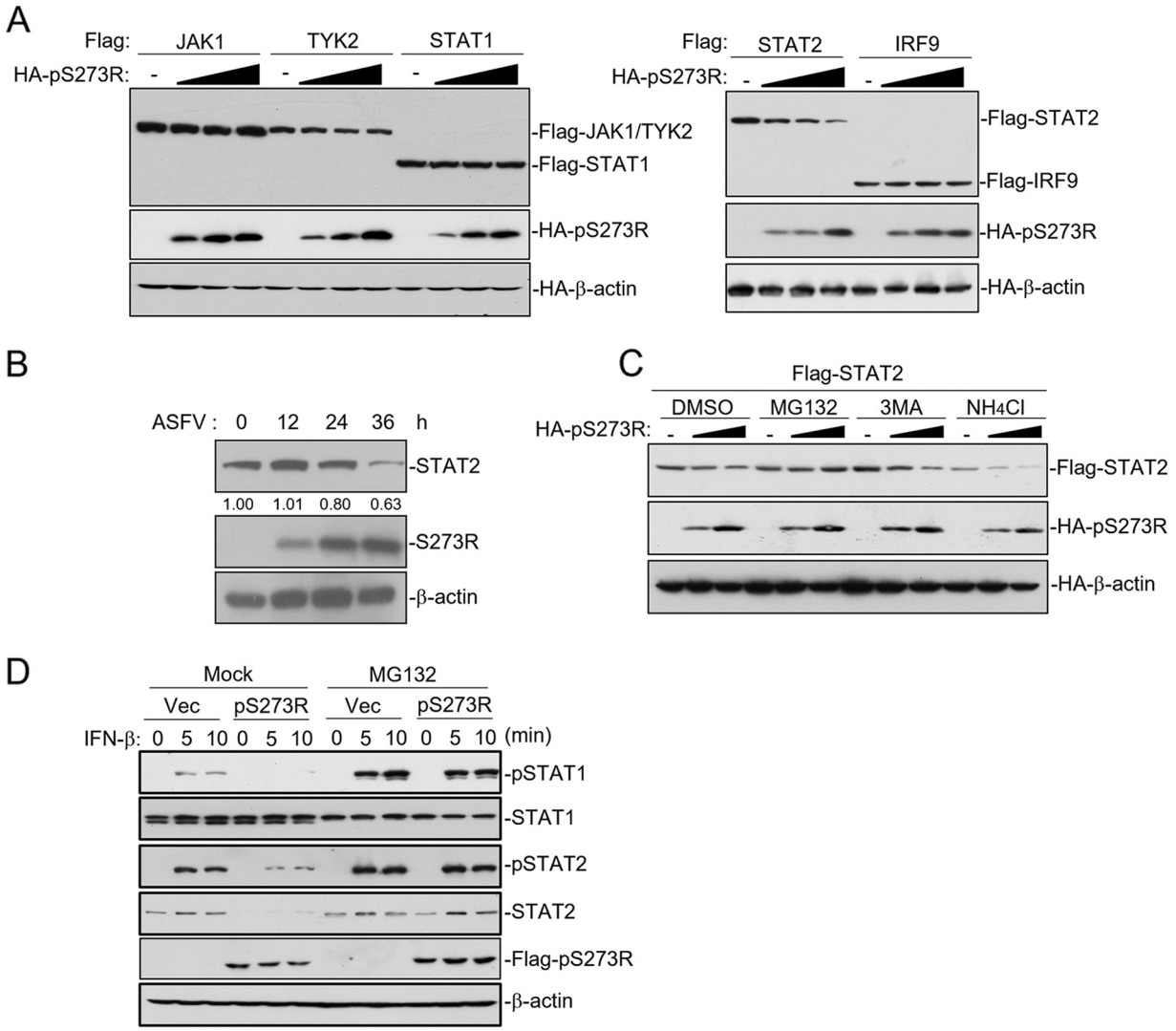

FIG 3 ASFV pS273R induces STAT2 degradation through the proteasomal pathway. (A) HEK293T cells (5×10^5) were transfected with plasmids of Flag-tagged JAK1 (0.3 μg), Flag-tagged TYK2 (0.3 μg), Flag-tagged STAT1 (0.3 μg), Flag-tagged STAT2 (0.3 μg), Flag-tagged IRF9 (0.3 μg), and increasing dose plasmids of HA-pS273R. Twenty-four hours later, cells were lysed and the expression levels of these proteins were determined by SDS-PAGE and Western blotting. β-Actin was used as a loading control. Data shown are representative of 3 repeated experiments. (B) PAMs (1×10^6) were infected with ASFV (MOI of 0.1) for 12 h, 24 h, or 36 h. Western blot assays were performed with the indicated antibodies. Data shown are representative of 2 repeated experiments. (C) HEK293T cells (5×10^5) were cotransfected with Flag-tagged pS273R and Flag-tagged STAT2. Twenty-four hours later, cells were left untreated or treated with MG132 (20 μM), 3MA (100 μM), or NH_4Cl (20 nM) for 6 h. Western blot assays were performed with the indicated antibodies. Data shown are representative of 2 repeated experiments. (D) HEK293T cells (5×10^5) were transfected with plasmids of Flag-tagged pS273R (1 μg). Twenty-four hours later, cells were treated or not treated with MG132 (20 μM) for 6 h before being stimulated with IFN-β (20 μM) for 0, 5, or 10 min. The phosphorylation and expression levels of the indicated proteins were examined by Western blotting. β-Actin was used as a loading control. Data shown are representative of 3 repeated experiments. DMSO, dimethyl sulfoxide.

PK-15 cells (Fig. 4E). Consistently, ASFV infection-induced degradation of STAT2 was restored by knockdown of DCST1 (Fig. 4F), suggesting that pS273R inhibits type I IFN signaling via DCST1. In addition, knockdown of DCST1 inhibited ASFV replication (see Fig. S3). Taken together, these results suggested that pS273R recruited the E3 ubiquitin ligase DCST1, which mediated K48-linked polyubiquitination of STAT2, thus impairing host antiviral responses.

DCST1-mediated polyubiquitination of STAT2 at K55 is responsible for pS273R-induced STAT2 degradation. Next, we further investigated DCST1-mediated ubiquitination of STAT2. Overexpression of DCST1 enhanced K48-linked polyubiquitination of STAT2. Domain mapping further suggested that, while DCST1 markedly enhanced polyubiquitination of the N terminus of STAT2 (STAT2-ND), it showed no

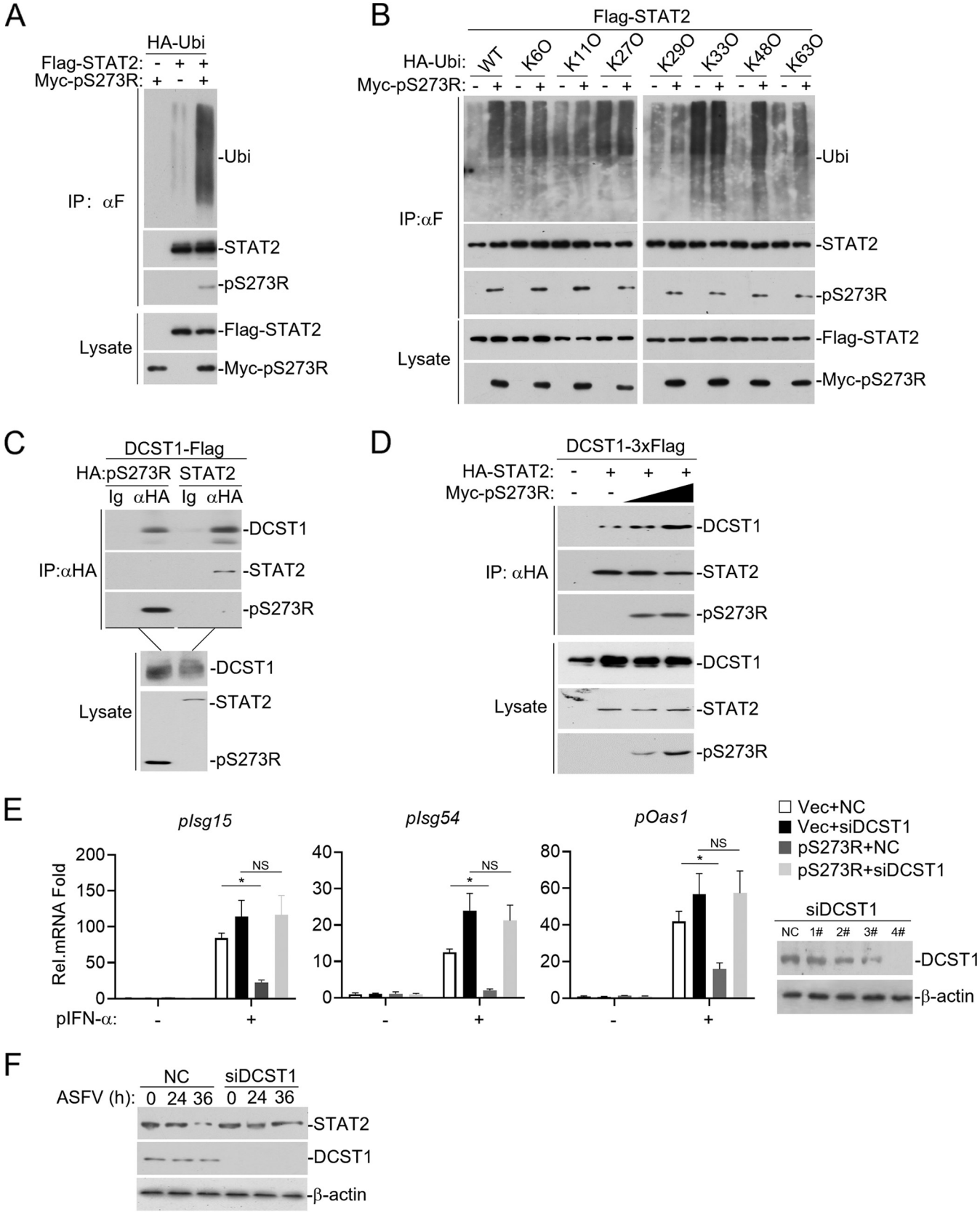

FIG 4 ASFV pS273R recruits the E3 ubiquitin ligase DCST1 and enhances K48-linked polyubiquitination of STAT2. (A) HEK293T cells (1×10^6) were cotransfected with Myc-tagged pS273R (1 μg), Flag-tagged STAT2 (2 μg) and HA-tagged ubiquitin (1 μg). Twenty-four hours later, cells were treated with

(Continued on next page)

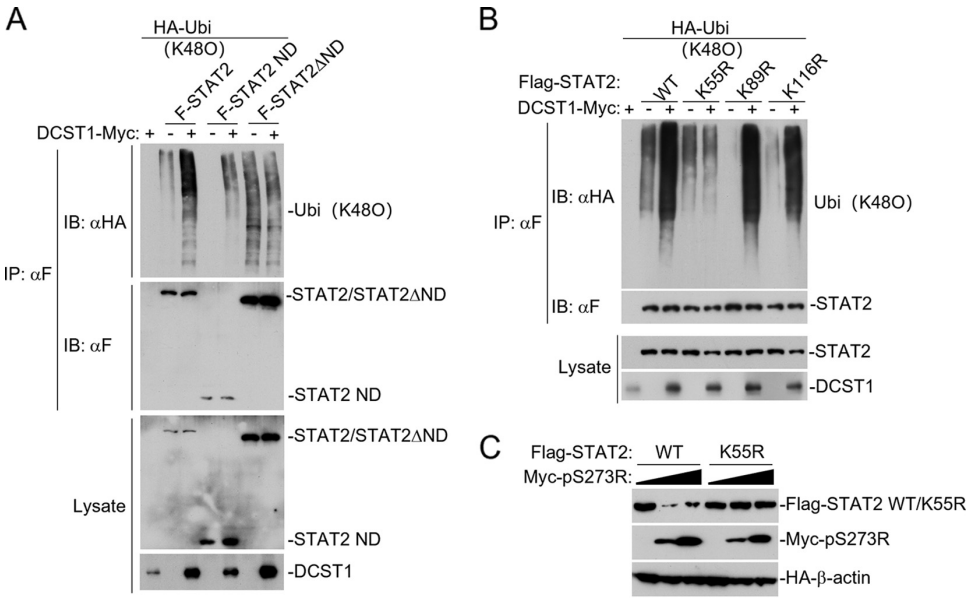

FIG 5 DCST1-mediated polyubiquitination at K55 of STAT2 is responsible for its degradation. (A) HEK293T cells (1×10^6) were cotransfected with Myc-tagged DCST1 (1 μg), Flag-tagged STAT2 (2 μg), Flag-STAT2-ND (2 μg), Flag-STAT2ΔND (2 μg), and HA-tagged K48O ubiquitin (2 μg). Twenty-four hours later, cells were treated with MG132 (20 μM) for 6 h. Coimmunoprecipitation (IP) and immunoblotting (IB) were performed with the indicated antibodies. Data shown are representative of 2 repeated experiments. (B) HEK293T cells (5×10^6) were cotransfected with HA-tagged K48O ubiquitin (2 μg), Flag-tagged STAT2 and mutants (2 μg), and Myc-tagged DCST1 (1 μg). Twenty-four hours later, cells were treated with MG132 (20 μM) for 6 h. Coimmunoprecipitation and immunoblotting were performed with the indicated antibodies. Data shown are representative of 3 repeated experiments. (C) HEK293T cells (5×10^5) were transfected with plasmids of Flag-STAT2 (0.3 μg), Flag-STAT2 K55R mutant (0.3 μg), and increasing dose plasmids of Myc-pS273R. Twenty-four hours later, cells were lysed, and the expression levels of these proteins were examined by SDS-PAGE and Western blotting. β-Actin was used as a loading control. Data shown are representative of 2 repeated experiments. WT, wild-type.

obvious effects on K48-linked polyubiquitination of STAT2ΔND (Fig. 5A), suggesting that the site of polyubiquitination is located in the N terminus of STAT2. To further determine the site of STAT2 polyubiquitination, we generated K55R, K89R, and K116R mutants of STAT2, in which three lysines in STAT2-ND were replaced with arginines. As shown in Fig. 5B, while DCST1 enhanced K48-linked polyubiquitination of the K89R and K116R mutants of STAT2, it failed to mediate K48-linked polyubiquitination of STAT2-K55R, indicating that K55 of STAT2 is the site of polyubiquitination by DCST1 (Fig. 5B). Interestingly, the STAT2-K55R mutant was resistant to pS273R-mediated degradation (Fig. 5C). Taken together, these results suggested that DCST1-mediated K48-linked polyubiquitination of STAT2 at K55 is responsible for pS273R-induced STAT2 degradation.

ASFV pS273R inhibits JAK-STAT signaling independently of its protease activity. ASFV pS273R is a cysteine protease that preferentially cleaves proteins with Gly-Gly-X amino acid motifs. Previous studies reported that the AD (amino acids 1 to 83), as well

FIG 4 Legend (Continued)

MG132 (20 μM) for 6 h. Coimmunoprecipitation (IP) and immunoblotting were performed with the indicated antibodies. Data shown are representative of 5 repeated experiments. (B) HEK293T cells (1×10^6) were cotransfected with Myc-tagged pS273R (1 μg), Flag-tagged STAT2 (2 μg) and different types of HA-tagged ubiquitin (1 μg). Twenty-four hours later, cells were treated with MG132 (20 μM) for 6 h. Coimmunoprecipitation and immunoblotting were performed with the indicated antibodies. Data shown are representative of 3 repeated experiments. (C) HEK293T cells (5×10^6) were cotransfected with Flag-tagged DCST1 (5 μg), HA-tagged pS273R (5 μg), and HA-tagged STAT2 (5 μg). Coimmunoprecipitation and immunoblotting were performed with the indicated antibodies. Data shown are representative of 2 repeated experiments. (D) HEK293T cells (5×10^6) were cotransfected with Myc-tagged pS273R, HA-tagged STAT2, and Flag-tagged DCST1. Coimmunoprecipitation and immunoblotting were performed with the indicated antibodies. Data shown are representative of 2 repeated experiments. (E) PK-15 cells stably expressing pS273R (1×10^6) were transfected with #4 siRNAs for porcine DCST1. Forty-eight hours later, cells were stimulated with porcine IFN-α (400 U) for 6 h. The *Isg15*, *Isg54*, and *Oas1* mRNA levels were analyzed by RT-qPCR. Student's *t* test was used for statistical analysis for means and average deviations. Data shown are representative of 2 repeated experiments. (F) PAMs (1×10^6) were transfected with control (NC) or DCST1 siRNAs. Forty-eight hours later, cells were infected with ASFV (MOI of 0.1) for 24 h or 36 h before Western blot assays were performed with the indicated antibodies. Data shown are representative of 2 repeated experiments.

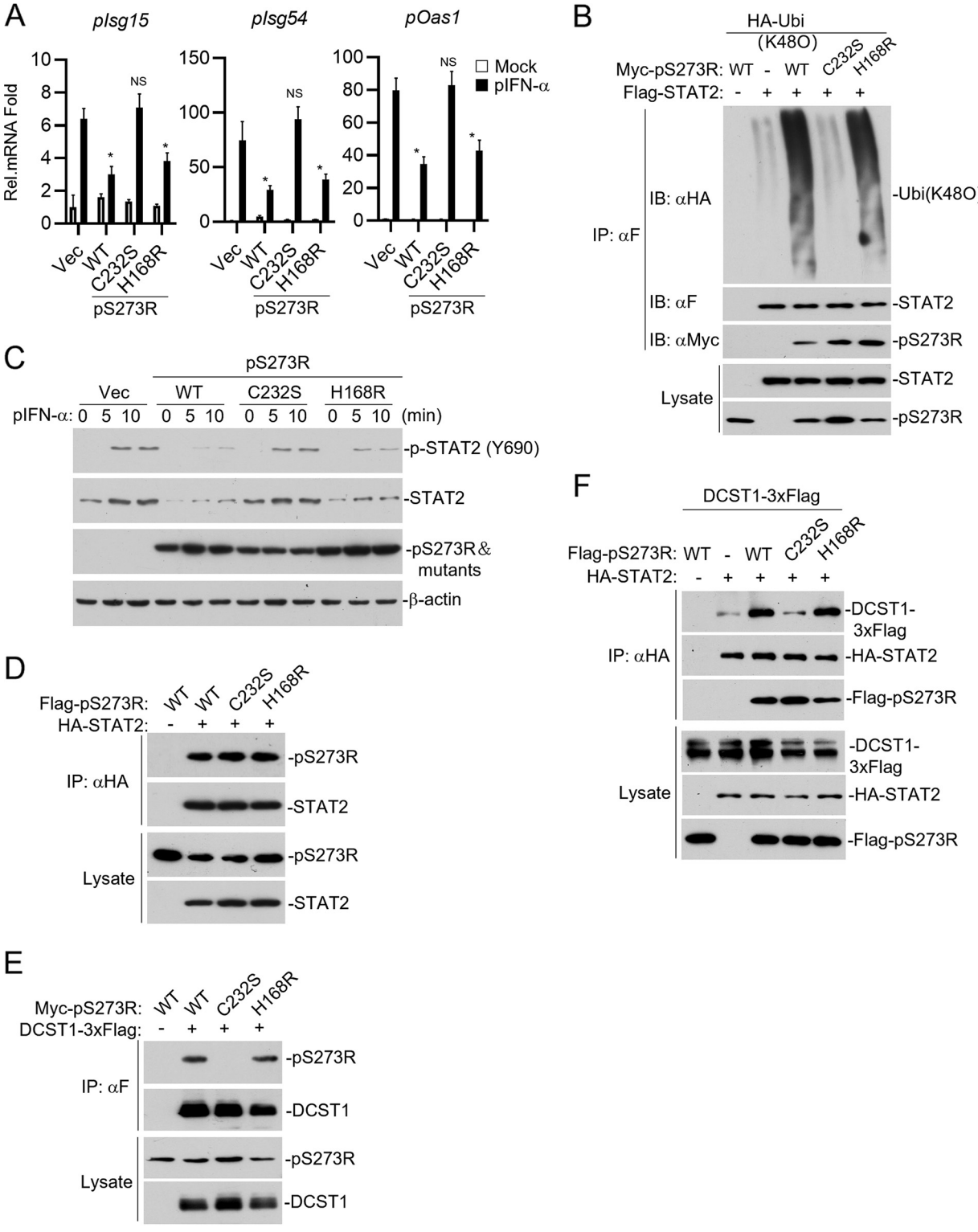

FIG 6 ASFV pS273R inhibits JAK-STAT signaling independently of its protease activity. (A) PK-15 cells (1×10^6) stably expressing wild-type (WT) and H168R and C232S mutants of pS273R were stimulated with porcine IFN-α (400 U) for 6 h. The mRNA levels of *pISG15*, *pISG54*, and p*oas1* were analyzed by RT-qPCR. One-way ANOVA was used for statistical analysis for means and average deviations. Data shown are representative of 2 repeated experiments. (B) HEK293T cells (1×10^6) were cotransfected with Myc-tagged wild-type and H168R and C232S mutants of pS273R (1 μg), Flag-tagged STAT2 (2 μg), and HA-tagged K48O ubiquitin (2 μg). Twenty-four hours later, cells were treated with MG132 (20 μM) for 6 h. Coimmunoprecipitation (IP) and immunoblotting (IB) were performed with the indicated antibodies. Data shown are representative of 3 repeated experiments. (C) PK-15 cells (5×10^6) stably expressing wild-type and H168R and C232S mutants of pS273R were stimulated with porcine IFN-α (400 U) for 0, 5, or 10 min. The phosphorylation and expression levels of the indicated proteins were

(Continued on next page)

as His168 and Cys232, of pS273R are essential for its protease activity. Depletion of the AD or mutation of either H168 or C232 resulted in loss of the protease activity of pS273R (14). We next determined whether the protease activity of pS273R is required for its regulation of type I IFN signaling. Interestingly, pS273R CD still showed an inhibitory effect on IFN-β-triggered STAT1/2 activation (Fig. 2G). In addition, while wild-type pS273R and pS273R(H168R) still inhibited transcription of *Isg15*, *Isg54*, and *Oas1* induced by IFN-α, pS273R(C232S) lost its inhibitory function (Fig. 6A). Consistently, pS273R(H168R) also enhanced K48-linked polyubiquitination and induced the degradation of STAT2 (Fig. 6B and C). Since the two enzymatically inactive mutants of pS273R still inhibited JAK-STAT signaling, we speculated that the protease activity of pS273R is not required for its inhibition of type I IFN signaling.

We next tried to elucidate why pS273R(C232S) lost its inhibitory function. We found that, while both H168R and C232S mutations of pS273R showed no effect on the interaction with STAT2 (Fig. 6D), pS273R(C232S) no longer interacted with DCST1 (Fig. 6E). Consistently, pS273R(C232S) failed to enhance the interaction between DCST1 and STAT2 (Fig. 6F), as well as the K48-linked polyubiquitination of STAT2 (Fig. 6B), indicating that mutation of Cys232 disabled pS273R from recruiting DCST1 to STAT2. Taken together, these results suggested that the ability to facilitate the DCST1-STAT2 interaction instead of the cysteine protease activity is critical for pS273R to antagonize type I IFN signaling.

DISCUSSION

The ASFV genome encodes more than 150 viral proteins. Previous studies have reported that ASFV has developed series of strategies to evade host antiviral responses, such as reducing IFN production, inhibiting IFN signaling, inhibiting infection-induced apoptosis, and disturbing inflammatory responses (10, 18–20). In this study, we identified pS273R as a new inhibitor of type I IFN signaling by genome-wide screening of ASFV-encoded proteins.

Several lines of evidence suggest that ASFV pS273R antagonizes type I IFN signaling by inducing DCST1-mediated ubiquitination and degradation of STAT2. First, overexpression of pS273R caused STAT2 degradation and inhibited IFN-β-triggered transcription of downstream ISGs. Second, pS273R interacted with STAT2 and enhanced the interaction between STAT2 and DCST1, which is an E3 ligase and has been reported to mediate K48-linked polyubiquitination of STAT2. Third, pS273R mutants that lost the ability to bridge the STAT2-DCST1 interaction failed to inhibit type I IFN-induced signaling. Fourth, pS273R-mediated STAT2 degradation was restored in DCST1 knockdown cells. In addition, the STAT2-K55R mutant, in which the ubiquitination site of DCST1 was mutated, was resistant to pS273R-mediated degradation. Taken together, these findings suggest that, following ASFV infection, the viral protein pS273R interacts with STAT2 and recruits the E3 ubiquitin ligase DCST1, which mediates ubiquitination of STAT2 and subsequently results in STAT2 degradation. ASFV pS273R-mediated STAT2 degradation leads to inhibition of ISG transcription induced by type I IFNs and thus antagonizes host antiviral innate immune responses.

ASFV pS273R has been reported to have protease activity, which processes viral polyprotein precursors to mature structural proteins required for virus assembly (13). Recently, it was reported that pS273R could inhibit infection-induced pyroptosis by noncanonically

FIG 6 Legend (Continued)
examined by Western blotting. Data shown are representative of 2 repeated experiments. (D) HEK293T cells (5×10^6) were cotransfected with Flag-tagged wild-type and H168R and C232S mutants of pS273R (1 μg) and HA-tagged STAT2 (2 μg). Coimmunoprecipitation and immunoblotting were performed with the indicated antibodies. Data shown are representative of 2 repeated experiments. (E) HEK293T cells (5×10^6) were cotransfected with Myc-tagged wild-type and H168R and C232S mutants of pS273R (1 μg) and Flag-tagged DCST1 (2 μg). Coimmunoprecipitation and immunoblotting were performed with the indicated antibodies. Data shown are representative of 2 repeated experiments. (F) HEK293T cells (5×10^6) were cotransfected with Flag-tagged wild-type and H168R and C232S mutants of pS273R (1 μg), HA-tagged STAT2 (2 μg), and Flag-tagged DCST1 (1 μg). Twenty-four hours later, cells were treated with MG132 (20 μM) for 6 h. Coimmunoprecipitation and immunoblotting were performed with the indicated antibodies. Data shown are representative of 3 repeated experiments.

cleaving gasdermin D, leading to antagonization of host antiviral responses (19). In our study, pS273R(H168R) and pS273R(CD), two catalytically inert mutants of pS273R, inhibited type I IFN signaling similarly as the wild-type pS273R, indicating that the protease activity of pS273R is dispensable for it to negatively regulate type I IFN signaling. These findings reveal a protease-independent function of pS273R in immune evasion.

The best way to elucidate the function of pS273R is to construct pS273R-deficient ASFV and test its replication and immune evasion in the course of infection. However, given that pS273R is required for the maturation of viral structural proteins and is necessary for ASFV replication (13), it is difficult to obtain pS273R-deficient viruses. In our study, we found that the ability to facilitate DCST1-STAT2 interaction instead of the cysteine protease activity is critical for pS273R to antagonize type I IFN signaling, which provides a possible strategy to generate a mutant virus by replacing pS273R with a mutant that loses the ability to facilitate DCST1-STAT2 interaction. It will be of interest to test the immune evasion ability of such a ASFV mutant in future studies.

Type I IFNs play important roles in host antiviral responses. Therefore, it is not surprising that viruses have evolved various mechanisms to antagonize type I IFNs for immune evasion. For example, herpes simplex virus type 1 (HSV-1) ICP0 inhibits IFN-induced ISG expression, and mutant virus deficient in ICP0 replicates less efficiently in host cells (21). Human cytomegalovirus miR-US33as-5p causes the degradation of IFN-α/β receptor 1 (IFNAR1) mRNA and thus inhibits the antiviral effects of type I IFNs (22). Hepatitis B virus Pol impairs phosphorylation of STAT1 at Ser727 to inhibit translocation of STAT1 to the nucleus (23). Previously, it has been reported that ASFV multiple gene family (MGF) proteins have immune evasion functions. For example, MGF360 and MGF505 have been reported to inhibit type I IFN-mediated antiviral effects, as ASFV isolates that possess MGF360/MGF505 were partially resistant to type I IFN treatment (20). In our screening, several candidate ASFV proteins were identified as potential inhibitors of type I IFN signaling, among which is pS273R. It is possible that ASFV, like other large DNA viruses, possesses multiple complementary and perhaps redundant mechanisms to target type I IFN responses.

In summary, our findings reveal a protease-independent function of ASFV pS273R in regulating host immune responses. pS273R bridges the interaction between STAT2 and the E3 ubiquitin ligase DCST1, which induces degradation of STAT2 and impaired type I IFN-mediated antiviral effects. The findings that ASFV pS273R not only is required for maturation of viral structural proteins but also is involved in evasion of host innate immune responses make it a potential target for the development of control measures against ASFV.

MATERIALS AND METHODS

Reagents, antibodies, viruses, and cells. The following reagents and antibodies were purchased from the indicated manufactures: dual-specificity luciferase assay kit (Promega), SYBR green (Bio-Rad), Polybrene (Millipore), RNase A (Thermo Fisher Scientific), human IFN-γ and IFN-β (R&D Systems), porcine IFN-α (PBL), puromycin (Thermo Fisher Scientific), Lipofectamine 2000 (Invitrogen), MG132 (MCE), 3MA (MCE), mouse antibodies against the hemagglutinin (HA) tag (BioLegend), Flag tag (Sigma), Myc tag (Cell Signaling Technology), and β-actin (Sigma), anti-phospho-JAK1 (Tyr1022) (Cell Signaling Technology), anti-phospho-TYK2 (Tyr1054) (Cell Signaling Technology), anti-phospho-STAT1 (Tyr701) (Cell Signaling Technology), anti-phospho-STAT2 (Tyr689/690) (Cell Signaling Technology), anti-JAK1 (Cell Signaling Technology), anti-TYK2 (Cell Signaling Technology), anti-STAT1 (Cell Signaling Technology), anti-STAT2 (Cell Signaling Technology), and anti-DCST1 (Abcam). Anti-pS273R antibody was generated by immunizing rabbits or mice with purified recombinant pS273R in the Center for Animal Experiment, Wuhan Institute of Virology, Chinese Academy of Sciences. The ASFV CN/GS/2018 strain was propagated on PAMs as described previously (24), by the African Swine Fever Regional Laboratory at the Lanzhou Veterinary Research Institute. HEK293T, PK-15 cells were purchased from ATCC. PAMs were prepared by bronchoalveolar lavage as described previously. PAMs were cultured at 37°C with 5% CO_2 in RPMI 1640 medium (Gibco) supplemented with 10% fetal bovine serum (Gibco) and 1% penicillin-streptomycin (Thermo Fisher Scientific).

Constructs. Mammalian protein-expressing plasmids were constructed in the pCMV14 or pRK vector by standard molecular biology methods. The point mutation plasmids were constructed by site-directed mutagenesis as described previously. Expression plasmids for JAK1, TYK2, STAT1, STAT2, IRF9, DCST1, FBXW7, and PDLIM2 were described previously. Expression plasmids for ASFV open reading frames (ORFs) were constructed by insertion of synthetic cDNA for particular ORFs into the pCMV7.1 vector as described previously (24).

Expression screen assays. HEK293T cells (1×10^5) were transfected with an expression plasmid for ASFV ORF (0.1 μg) and the STAT1/2 promoter luciferase reporter plasmid (0.05 μg) by the standard calcium phosphate precipitation method. To normalize for transfection efficiency, 0.01 μg of pRL-TK (*Renilla* luciferase) reporter plasmid was included in each transfection. Twenty-four hours later, cells were further stimulated with IFN-β (20 μM) for 10 h before luciferase assays were performed using a dual-specificity luciferase assay kit (Promega) according to the manufacturer's instructions.

Coimmunoprecipitation and immunoblotting analyses. Cells were lysed in NP-40 lysis buffer (20 mM Tris-HCl [pH 7.4], 150 mM NaCl, 1 mM EDTA, and 1% NP-40) supplemented with protease and phosphatase inhibitors. For each immunoprecipitation, 400 μL of cell lysate was incubated at 4°C for 2 h with 0.5 μg of the indicated antibodies and 30 μL of a 50% slurry of protein G-Sepharose (GE Healthcare). The Sepharose beads were then washed three times with 1 mL of lysis buffer containing 500 mM NaCl. The precipitates were resuspended with 50 μL 2× SDS loading buffer and boiled for 10 min. Immunoblotting analysis was performed following standard procedures.

Pulldown assay. pET-30c-STAT2 and pGEX-6p-1-pS273R were expressed in the *Escherichia coli* Rosetta strain. Recombinant glutathione *S*-transferase (GST)-pS273R protein was purified with glutathione-Sepharose. Purified His-STAT2 protein was added to the glutathione-Sepharose coupled with recombinant GST-pS273R and incubated for 3 h at 4°C in NP-40 lysis buffer. Subsequently, the beads were washed in 1 mL of NP-40 lysis buffer containing 500 mM NaCl and boiled with 50 μL 2× SDS loading buffer. The eluates/input were resolved by SDS-PAGE and detected by Coomassie staining and immunoblotting.

RNA extraction and qPCR. Total RNA was extracted using the TRIzol reagent according to the procedures suggested by the manufacturer. cDNA was synthesized using an oligo(dT) primer and Moloney murine leukemia virus (M-MLV) reverse transcriptase (Invitrogen). qPCR analysis was performed to measure the mRNA abundance of the indicated genes. Data shown are the relative abundance of the indicated mRNA normalized to that of glyceraldehyde-3-phosphate dehydrogenase (GAPDH). The sequences of qPCR primer pairs were as reported previously or as follows: porcine *Gapdh*, 5′-ACATGGCCTCCAAGGAGTAAGA-3′ and 5′-GATCGAGTTGGGGCTGTGACT-3′; porcine *Isg15*, 5′-CCTGTTGATGGTGCAAAGCT-3′ and 5′-TGCACATAGGCTTGAGGTCA-3′; porcine *Isg54*, 5′-CTGGCAAAGAGCCCTAAGGA-3′ and 5′-CTCAGAGGGTCAATGGAATTCC-3′; porcine *Oas1*, 5′-AAGCATCAGAAGCTTTGCATCTT-3′ and 5′-CAGGCCTGGGTTTCTTGAGTT-3′; porcine *Mx1*, 5′-TCTGTAAGCAGGAGACCATCAACT-3′ and 5′-TTTCTCGCCACGTCCACTATC-3′; human *GAPDH*, 5′-GACAAGCTTCCCGTTCTCAG-3′ and 5′-GAGTCAACGGATTTGGTCGT-3′; human *ISG15*, 5′-AGGACAGGGTCCCCCTTGCC-3′ and 5′-CCTCCAGCCCGCTCACTTGC-3′; human *ISG54*, 5′-GGAGCAGATTCTGAGGCTTTGC-3′ and 5′-GGATGAGGCTTCCAGACTCCAA-3′; human *ISG56*, 5′-TCATCAGGTCAAGGATAGTC-3′ and 5′-GCCACACTGTATTTGGTGTCTAGG-3′; ASFV *p72*, 5′-CCGGGTACAATGGGTCTTCC-3′ and 5′-CGCAACGGATATGACTGGGA-3′.

Confocal microscopy. PAMs were infected with the ASFV CN/GS/2018 strain (multiplicity of infection [MOI] of 0.2) for 12 or 24 h, fixed with 4% paraformaldehyde for 24 h, and permeabilized with 0.1% Triton X-100 in phosphate-buffered saline (PBS) for 10 min at 4°C. The cells were blocked with 1% bovine serum albumin (BSA) in PBS and incubated with anti-STAT2 (Cell Signaling Technology) and anti-pS273R for 8 h and with the secondary antibodies for 1 h. The nuclei were stained with 4′,6-diamidino-2-phenylindole (DAPI). The cells were observed with a Nikon confocal microscope with a 60× objective.

RNA interference. Small interfering RNA (siRNA) duplexes targeting porcine DCST1 were chemically synthesized by Gene-Pharma. The siRNA duplexes (50 nM) were transfected into cells using the PepMute siRNA transfection reagent (SignaGen Laboratories) according to the manufacturer's instructions. Six hours after transfection, the medium was replaced with fresh medium and cells were further incubated for 42 h. The sequences of the siRNA oligonucleotides are as follows: siDcst1-#1, 5′-CCUGGCCAUAGGUCUCUUUdTdT-3′; siDcst1-#2, 5′-GCCUGCCCAUGAAGUUCAAdTdT-3′; siDcst1-#3, 5′-CCUGCCCAUGAAGUUCAAAdTdT-3′; siDcst1-#4, 5′-CCUUCCUGCAGUACUCCUUdTdT-3′.

Virus titration. The ASFV CN/GS/2018 strain was quantified by using hemadsorption (HAD) assays as described previously, with minor modifications (25). In brief, PAMs were seeded in 96-well plates. The samples were then added to the plates and titrated in triplicate using 10-fold serial dilutions. HAD was determined at day 7 postinoculation, and 50% HAD doses (HAD_{50}) were calculated by using the Reed-Muench method.

Biosafety statement and facility. All experiments with live ASFV were conducted within the enhanced biosafety level 3 facilities in the Lanzhou Veterinary Research Institute, Chinese Academy of Agricultural Sciences. The principles and procedures have been approved by the Ministry of Agriculture and Rural Affairs and the China National Accreditation Service for Conformity Assessment.

Statistical analysis. For two sets of samples, paired, two-tailed Student's *t* test was used for statistical analysis and the F test was performed to confirm that the two populations had the same variances. For multiple comparisons, one-way analysis of variance (ANOVA) was performed, followed by a *post hoc* test. Statistical differences were evaluated using GraphPad Prism software. Data are presented as mean ± average deviation.

SUPPLEMENTAL MATERIAL

Supplemental material is available online only.

SUPPLEMENTAL FILE 1, PDF file, 0.5 MB.

ACKNOWLEDGMENTS

We thank Fan Zhang and You-ling Zhu at the Center for Experimental Animals, Wuhan Institute of Virology, for their help with the generation of the anti-pS273R antibody.

This study was supported by the African Swine Fever Research Emergency Program of the Chinese Academy of Sciences (grant KJZD-SW-L06) and the National Nature Science Foundation of China (grant U20A2059).

REFERENCES

1. Montgomery RE. 1921. On a form of swine fever occurring in British East Africa (Kenya Colony). J Comp Pathol Ther 34:159–191. https://doi.org/10.1016/S0368-1742(21)80031-4.
2. Sauter-Louis C, Conraths FJ, Probst C, Blohm U, Schulz K, Sehl J, Fischer M, Forth JH, Zani L, Depner K, Mettenleiter TC, Beer M, Blome S. 2021. African swine fever in wild boar in Europe: a review. Viruses 13:1717. https://doi.org/10.3390/v13091717.
3. Wang F, Zhang H, Hou L, Yang C, Wen Y. 2021. Advance of African swine fever virus in recent years. Res Vet Sci 136:535–539. https://doi.org/10.1016/j.rvsc.2021.04.004.
4. Dixon LK, Stahl K, Jori F, Vial L, Pfeiffer DU. 2020. African swine fever epidemiology and control. Annu Rev Anim Biosci 8:221–246. https://doi.org/10.1146/annurev-animal-021419-083741.
5. Blome S, Franzke K, Beer M. 2020. African swine fever: a review of current knowledge. Virus Res 287:198099. https://doi.org/10.1016/j.virusres.2020.198099.
6. Fraczyk M, Woźniakowski G, Kowalczyk A, Bocian Ł, Kozak E, Niemczuk K, Pejsak Z. 2016. Evolution of African swine fever virus genes related to evasion of host immune response. Vet Microbiol 193:133–144. https://doi.org/10.1016/j.vetmic.2016.08.018.
7. Grigoriu S, Bond R, Cossio P, Chen JA, Ly N, Hummer G, Page R, Cyert MS, Peti W. 2013. The molecular mechanism of substrate engagement and immunosuppressant inhibition of calcineurin. PLoS Biol 11:e1001492. https://doi.org/10.1371/journal.pbio.1001492.
8. Correia S, Ventura S, Parkhouse RM. 2013. Identification and utility of innate immune system evasion mechanisms of ASFV. Virus Res 173:87–100. https://doi.org/10.1016/j.virusres.2012.10.013.
9. Ran Y, Li D, Xiong M-G, Liu H-N, Feng T, Shi Z-W, Li Y-H, Wu H-N, Wang S-Y, Zheng H-X, Wang Y-Y. 2022. African swine fever virus I267L acts as an important virulence factor by inhibiting RNA polymerase III-RIG-I-mediated innate immunity. PLoS Pathog 18:e1010270. https://doi.org/10.1371/journal.ppat.1010270.
10. Wang X, Wu J, Wu Y, Chen H, Zhang S, Li J, Xin T, Jia H, Hou S, Jiang Y, Zhu H, Guo X. 2018. Inhibition of cGAS-STING-TBK1 signaling pathway by DP96R of ASFV China 2018/1. Biochem Biophys Res Commun 506:437–443. https://doi.org/10.1016/j.bbrc.2018.10.103.
11. Stark GR, Darnell JE, Jr. 2012. The JAK-STAT pathway at twenty. Immunity 36:503–514. https://doi.org/10.1016/j.immuni.2012.03.013.
12. Zsak L, Lu Z, Burrage TG, Neilan JG, Kutish GF, Moore DM, Rock DL. 2001. African swine fever virus multigene family 360 and 530 genes are novel macrophage host range determinants. J Virol 75:3066–3076. https://doi.org/10.1128/JVI.75.7.3066-3076.2001.
13. Andrés G, Alejo A, Simón-Mateo C, Salas ML. 2001. African swine fever virus protease, a new viral member of the SUMO-1-specific protease family. J Biol Chem 276:780–787. https://doi.org/10.1074/jbc.M006844200.
14. Li G, Liu X, Yang M, Zhang G, Wang Z, Guo K, Gao Y, Jiao P, Sun J, Chen C, Wang H, Deng W, Xiao H, Li S, Wu H, Wang Y, Cao L, Jia Z, Shang L, Yang C, Guo Y, Rao Z. 2020. Crystal structure of African swine fever virus pS273R protease and implications for inhibitor design. J Virol 94:e02125-19. https://doi.org/10.1128/JVI.02125-19.
15. Lee C-J, An H-J, Kim S-M, Yoo S-M, Park J, Lee G-E, Kim W-Y, Kim DJ, Kang HC, Lee JY, Lee HS, Cho S-J, Cho Y-Y. 2020. FBXW7-mediated stability regulation of signal transducer and activator of transcription 2 in melanoma formation. Proc Natl Acad Sci U S A 117:584–594. https://doi.org/10.1073/pnas.1909879116.
16. Joyce MA, Berry-Wynne KM, Dos Santos T, Addison WR, McFarlane N, Hobman T, Tyrrell DL. 2019. HCV and flaviviruses hijack cellular mechanisms for nuclear STAT2 degradation: up-regulation of PDLIM2 suppresses the innate immune response. PLoS Pathog 15:e1007949. https://doi.org/10.1371/journal.ppat.1007949.
17. Nair S, Bist P, Dikshit N, Krishnan MN. 2016. Global functional profiling of human ubiquitome identifies E3 ubiquitin ligase DCST1 as a novel negative regulator of type-I interferon signaling. Sci Rep 6:36179. https://doi.org/10.1038/srep36179.
18. García-Belmonte R, Pérez-Núñez D, Pittau M, Richt JA, Revilla Y. 2019. African swine fever virus Armenia/07 virulent strain controls interferon beta production through the cGAS-STING pathway. J Virol 93:e02298-18. https://doi.org/10.1128/JVI.02298-18.
19. Zhao G, Li T, Liu X, Zhang T, Zhang Z, Kang L, Song J, Zhou S, Chen X, Wang X, Li J, Huang L, Li C, Bu Z, Zheng J, Weng C. 2022. African swine fever virus cysteine protease pS273R inhibits pyroptosis by noncanonically cleaving gasdermin D. J Biol Chem 298:101480. https://doi.org/10.1016/j.jbc.2021.101480.
20. Gao Q, Yang Y, Quan W, Zheng J, Luo Y, Wang H, Chen X, Huang Z, Chen X, Xu R, Zhang G, Gong L. 2021. The African swine fever virus with MGF360 and MGF505 deleted reduces the apoptosis of porcine alveolar macrophages by inhibiting the NF-κB signaling pathway and interleukin-1β. Vaccines (Basel) 9:1371. https://doi.org/10.3390/vaccines9111371.
21. Everett RD, Parada C, Gripon P, Sirma H, Orr A. 2008. Replication of ICP0-null mutant herpes simplex virus type 1 is restricted by both PML and Sp100. J Virol 82:2661–2672. https://doi.org/10.1128/JVI.02308-07.
22. Zhang Q, Song X, Ma P, Lv L, Zhang Y, Deng J, Zhang Y. 2021. Human cytomegalovirus miR-US33as-5p targets IFNAR1 to achieve immune evasion during both lytic and latent infection. Front Immunol 12:628364. https://doi.org/10.3389/fimmu.2021.628364.
23. Chen J, Wu M, Zhang X, Zhang W, Zhang Z, Chen L, He J, Zheng Y, Chen C, Wang F, Hu Y, Zhou X, Wang C, Xu Y, Lu M, Yuan Z. 2013. Hepatitis B virus polymerase impairs interferon-α-induced STA T activation through inhibition of importin-α5 and protein kinase C-δ. Hepatology 57:470–482. https://doi.org/10.1002/hep.26064.
24. Li D, Liu Y, Qi X, Wen Y, Li P, Ma Z, Liu Y, Zheng H, Liu Z. 2021. African swine fever virus MGF-110-9L-deficient mutant has attenuated virulence in pigs. Virol Sin 36:187–195. https://doi.org/10.1007/s12250-021-00350-6.
25. Salguero FJ, Gil S, Revilla Y, Gallardo C, Arias M, Martins C. 2008. Cytokine mRNA expression and pathological findings in pigs inoculated with African swine fever virus (E-70) deleted on A238L. Vet Immunol Immunopathol 124:107–119. https://doi.org/10.1016/j.vetimm.2008.02.012.